

SHORT COMMUNICATION

A FOUR-NODE PLATE BENDING ELEMENT BASED ON MINDLIN/REISSNER PLATE THEORY AND A MIXED INTERPOLATION

KLAUS-JÜRGEN BATHE[†] AND EDUARDO N. DVORKIN[‡]

Massachusetts Institute of Technology, Cambridge, Massachusetts, U.S.A.

SUMMARY

This communication discusses a 4-node plate bending element for linear elastic analysis which is obtained, as a special case, from a general nonlinear continuum mechanics based 4-node shell element formulation. The formulation of the plate element is presented and the results of various example solutions are given that yield insight into the predictive capability of the plate (and shell) element.

INTRODUCTION

Since the development of the first plate bending finite elements, a very large number of elements has been proposed.^{1–3} These elements are usually developed and evaluated for the linear analysis of plates, but it is frequently implied that the elements can ‘easily’ be extended to the geometrically nonlinear analysis of general shell structures.

Our experiences are different. We believe that it can be a major step to extend a linear plate bending element formulation to obtain a general effective shell element, and with some plate element formulations this extension is (almost) not possible. Therefore, to obtain a general 4-node nonlinear shell element, we have concentrated directly on the development of such an element. As a special case, the shell element will then reduce to a plate bending element for the linear elastic analysis of plates.

Some results of our efforts to develop a general 4-node shell element were presented earlier.⁴ Our objective in this communication is to show how the general continuum mechanics based shell element formulation of Reference 4 reduces to an attractive plate bending analysis capability, and to give some more insight into our shell element formulation.

Considering the use of our shell element in the linear analysis of plates, there are at least two closely related plate bending element formulations—those presented by MacNeal⁵ and by Hughes and Tezduyar⁶—and there may be others because of the extensive recent developments—and the many possibilities—in displacement-based, hybrid and mixed formulations of linear plate bending elements.

Since our objective is to present a plate bending element formulation that is a special case of a general nonlinear 4-node shell element formulation,⁴ it is valuable to review briefly some thoughts that led to the development of the shell element. Our experience is that the high-order 16-node isoparametric degenerate shell element and the 3-node triangular discrete Kirchhoff plate/shell

[†]Professor of Mechanical Engineering.

[‡]Research Assistant.

element evaluated in References 7 and 8, are quite effective, but in some respects—for example, the cost and distortion sensitivity of the 16-node element and the low-order membrane stress predictive capability of the 3-node element—improvements are very desirable. We concluded therefore that it would be valuable to try to develop an efficient 4-node quadrilateral shell element based on the concepts of the degenerate isoparametric shell elements, the discrete Kirchhoff theory and the use of reduced constraints.^{2,9} The element should satisfy the usual isotropy and convergence requirements,² and more specifically:

1. The element should be formulated without use of a specific shell theory so that it is applicable to any plate/shell situation.
2. The element should not lock in thin plate/shell analyses.
3. The element should not contain any spurious zero energy modes.
4. The formulation should not be based on numerically adjusted factors.
5. The element should have good predictive capability for displacements, bending moments and membrane forces[†], and be relatively insensitive to element distortions.
6. The element should be simple and inexpensive to use with, for shell analysis, five or six engineering degrees-of-freedom per node, and for plate analysis three degrees-of-freedom per node.

As discussed in Reference 4, the essence of our element formulation lies in the separate interpolation of the transverse displacements/section rotations and of the transverse shear strains. The displacements and rotations are interpolated as usual, but for the transverse shear strains, the covariant components measured in the natural co-ordinate system are interpolated.

In the following sections, we first summarize the plate bending element formulation obtained from our general shell element formulation, and then briefly discuss its characteristics measured on the above objectives. This discussion includes the presentation of a number of analysis results on the problems that were considered by Batoz and Ben Tahar³ in their evaluation of quadrilateral plate bending elements[†]. This valuable reference contains a discussion of a large number of plate elements and may be used in a study of the results presented below.

FORMULATION OF THE ELEMENT

The plate element obtained from our general 4-node shell element is based on the Mindlin/Reissner plate theory and represents an extension of the formulation given in Reference 2, pp. 251–255. As presented there, the variational indicator of a Mindlin/Reissner plate is, in linear elastic static analysis,

$$\Pi = \frac{1}{2} \int_A \boldsymbol{\kappa}^T \mathbf{C}_b \boldsymbol{\kappa} dA + \frac{1}{2} \int_A \boldsymbol{\gamma}^T \mathbf{C}_s \boldsymbol{\gamma} dA - \int_A w p dA \quad (1)$$

where

$$\boldsymbol{\kappa} = \begin{bmatrix} \frac{\partial \beta_x}{\partial x} \\ \frac{\partial \beta_y}{\partial y} \\ \frac{\partial \beta_x}{\partial y} - \frac{\partial \beta_y}{\partial x} \end{bmatrix} \quad (2)$$

[†]An element with high predictive capability in transverse shear forces also, can probably be obtained by applying the procedures given in this paper and in Reference 4 to a higher-order element.

[‡]We have chosen not to compare our element to any other specific element, because ‘which one to choose?’

$$\gamma = \begin{bmatrix} \frac{\partial w}{\partial x} + \beta_x \\ \frac{\partial w}{\partial y} - \beta_y \end{bmatrix} \tag{3}$$

$$C_b = \frac{Eh^3}{12(1-\nu^2)} \begin{bmatrix} 1 & \nu & 0 \\ \nu & 1 & 0 \\ 0 & 0 & \frac{1-\nu}{2} \end{bmatrix}; \quad C_s = \frac{Ehk}{2(1+\nu)} \begin{bmatrix} 1 & 0 \\ 0 & 1 \end{bmatrix} \tag{4}$$

and, with reference to Figure 1, β_x, β_y are the section rotations, w is the transverse displacement of the mid-surface of the plate, p is the distributed pressure loading, h is the thickness of the plate (assumed constant) and A is the area of the mid-surface of the plate. Also, E is Young's modulus, ν is Poisson's ratio and k is a shear correction factor (appropriately set to 5/6).

Perhaps the simplest way to formulate an element based on the variational indicator Π in equation (1) is to interpolate both the transverse displacements and the section rotations as follows:

$$w = \sum_{i=1}^q h_i w_i \quad \beta_x = \sum_{i=1}^q h_i \theta_y^i, \quad \beta_y = \sum_{i=1}^q h_i \theta_x^i \tag{5}$$

where the w_i, θ_y^i and θ_x^i are the nodal point values of the variables w, β_x and β_y , respectively, the $h_i(r, s)$ are the interpolation functions and q is the number of element nodes. A basic problem inherent in the use of the above interpolations is that when q is equal to four, see Figure 2, the element 'locks' when it is thin (assuming 'full' numerical integration). This is due to the fact that with these interpolations the transverse shear strains cannot vanish at all points in the element when it is subjected to a constant bending moment. Hence, although the basic continuum mechanics equations contain the Kirchhoff plate assumptions, the finite element discretization is not able to represent these assumptions rendering the element not applicable to the analysis of thin plates or shells (see Reference 2, p. 240). To solve this deficiency, various remedies based on selective and reduced integration have been proposed, but there is still much room for a more effective and reliable approach.

To circumvent the locking problem, we formulate the element stiffness matrix in our approach by including the bending effects and transverse shear effects through different interpolations. To evaluate the section curvatures, κ , we use equation (2) and the interpolations in equation (5).

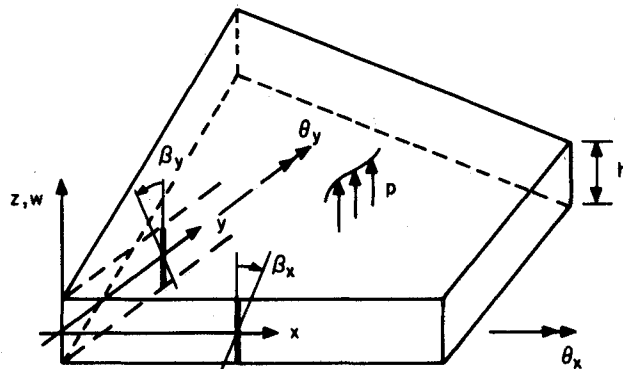


Figure 1. Notation used for Mindlin/Reissner plate theory

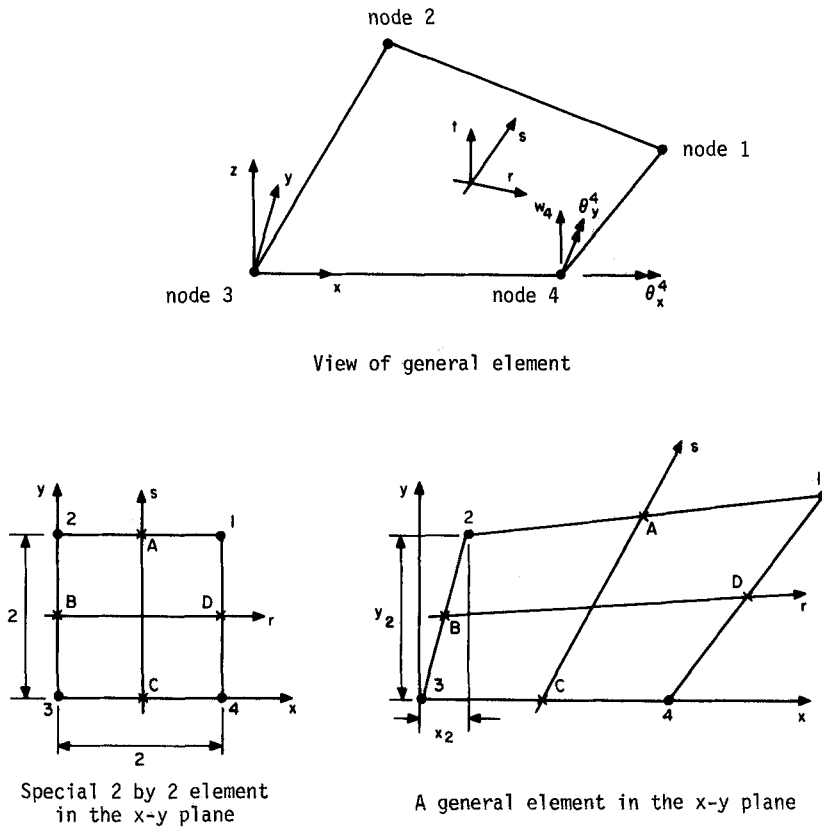


Figure 2. Conventions used in formulation of 4-node plate bending element: $h_1 = \frac{1}{4}(1+r)(1+s)$, $h_2 = \frac{1}{4}(1-r)(1+s)$, $h_3 = \frac{1}{4}(1-r)(1-s)$, $h_4 = \frac{1}{4}(1+r)(1-s)$

Hence, the element section curvatures are calculated as usual;² however, to evaluate the transverse shear strains we proceed differently.

Consider first our element when it is of geometry 2×2 (for which the (x, y) co-ordinates could be taken to be equal to the (r, s) isoparametric co-ordinates). For this element we use the interpolations

$$\begin{aligned} \gamma_{rz} &= \frac{1}{2}(1+s)\gamma_{rz}^A + \frac{1}{2}(1-s)\gamma_{rz}^C \\ \gamma_{sz} &= \frac{1}{2}(1+r)\gamma_{sz}^D + \frac{1}{2}(1-r)\gamma_{sz}^B \end{aligned} \tag{6}$$

where $\gamma_{rz}^A, \gamma_{rz}^C, \gamma_{sz}^D$ and γ_{sz}^B are the (physical) shear strains at points A, B, C , and D . We evaluate these strains using the interpolations in equation (5) to obtain

$$\gamma_{rz} = \frac{1}{2}(1+s) \left[\frac{w_1 - w_2}{2} + \frac{\theta_y^1 + \theta_y^2}{2} \right] + \frac{1}{2}(1-s) \left[\frac{w_4 - w_3}{2} + \frac{\theta_y^4 + \theta_y^3}{2} \right] \tag{7a}$$

and

$$\gamma_{sz} = \frac{1}{2}(1+r) \left[\frac{w_1 - w_4}{2} - \frac{\theta_x^1 + \theta_x^4}{2} \right] + \frac{1}{2}(1-r) \left[\frac{w_2 - w_3}{2} - \frac{\theta_x^2 + \theta_x^3}{2} \right] \tag{7b}$$

With these interpolations given, all strain-displacement interpolation matrices can directly be constructed and the stiffness matrix is formulated in the standard manner (see Reference 2, p. 252).

Considering next the case of a general 4-node element, we use the same basic idea of interpolating the transverse shear strains, but—using the interpolation of equation (6)—we interpolate the covariant tensor components measured in the (r, s) co-ordinate system. In this way we are directly taking account of the element distortion (from the 2×2 geometry). Proceeding this way with the tensor shear strain components we obtain—as shown in Appendix I—the following expressions for the γ_{xz} and γ_{yz} shear strains:

$$\gamma_{xz} = \gamma_{rz} \sin \beta - \gamma_{sz} \sin \alpha \quad (8a)$$

$$\gamma_{yz} = -\gamma_{rz} \cos \beta + \gamma_{sz} \cos \alpha \quad (8b)$$

where α and β are the angles between the r - and x -axis and s - and x -axis, respectively, and

$$\gamma_{rz} = \frac{\sqrt{[(C_x + rB_x)^2 + (C_y + rB_y)^2]}}{8 \det \mathbf{J}} \cdot \left\{ (1+s) \left[\frac{w_1 - w_2}{2} + \frac{x_1 - x_2}{4} (\theta_y^1 + \theta_y^2) - \frac{(y_1 - y_2)}{4} (\theta_x^1 + \theta_x^2) \right] + (1-s) \left[\frac{w_4 - w_3}{2} + \frac{x_4 - x_3}{4} (\theta_y^4 + \theta_y^3) - \frac{(y_4 - y_3)}{4} (\theta_x^4 + \theta_x^3) \right] \right\} \quad (9a)$$

$$\gamma_{sz} = \frac{\sqrt{[(A_x + sB_x)^2 + (A_y + sB_y)^2]}}{8 \det \mathbf{J}} \cdot \left\{ (1+r) \left[\frac{(w_1 - w_4)}{2} + \frac{x_1 - x_4}{4} (\theta_y^1 + \theta_y^4) - \frac{(y_1 - y_4)}{4} (\theta_x^1 + \theta_x^4) \right] + (1-r) \left[\frac{(w_2 - w_3)}{2} + \frac{(x_2 - x_3)}{4} (\theta_y^2 + \theta_y^3) - \frac{(y_2 - y_3)}{4} (\theta_x^2 + \theta_x^3) \right] \right\} \quad (9b)$$

In equations (9a) and (9b) we have

$$\det \mathbf{J} = \det \begin{bmatrix} \frac{\partial x}{\partial r} & \frac{\partial y}{\partial r} \\ \frac{\partial x}{\partial s} & \frac{\partial y}{\partial s} \end{bmatrix}$$

and

$$\begin{aligned} A_x &= x_1 - x_2 - x_3 + x_4 \\ B_x &= x_1 - x_2 + x_3 - x_4 \\ C_x &= x_1 + x_2 - x_3 - x_4 \\ A_y &= y_1 - y_2 - y_3 + y_4 \\ B_y &= y_1 - y_2 + y_3 - y_4 \\ C_y &= y_1 + y_2 - y_3 - y_4 \end{aligned} \quad (10)$$

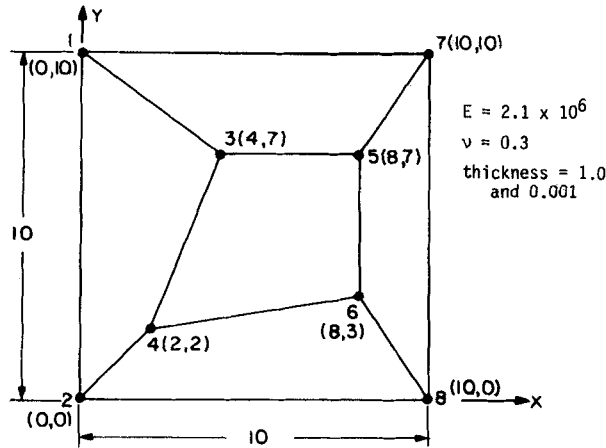
The formulation of the element can be regarded as a mixed formulation, in which the section rotations and transverse displacements are interpolated as given in equation (5), the curvatures are calculated using equation (2) and the shear strains are interpolated as shown above. In the interpolation, the intensities of the transverse shear strains are at the points A, B, C and D constrained to equal the transverse shear strains evaluated using equation (5). The element formulation can also be interpreted as based on a reduced penalty constraint between the

transverse displacements and the section rotations, or the element can be viewed as based on a 'discrete Mindlin/Reissner theory'.

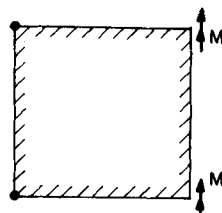
ELEMENT CHARACTERISTICS

Based on our studies, we find the following important element properties (assuming 'full' numerical integration over r and s):

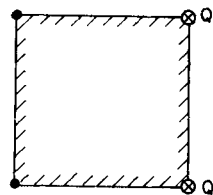
1. The element is able to represent the three rigid modes. The element contains the three rigid body



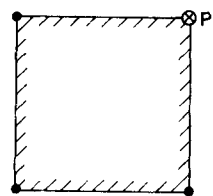
(a) Patch of elements used



Bending Case
 Boundary conditions:
 Node 1 $w = 0; \theta_y = 0$
 Node 2 $w = 0; \theta_y = 0$



Shearing Case
 Boundary conditions:
 At all nodes $\theta_x = 0; \theta_y = 0$
 Node 1 $w = 0$
 Node 2 $w = 0$



Twisting Case
 Boundary conditions:
 Node 1 $w = 0$
 Node 2 $w = 0$
 Node 8 $w = 0$

(b) Load cases

Figure 3. Patch test. A patch of elements is considered in the load cases shown; the patch test is passed

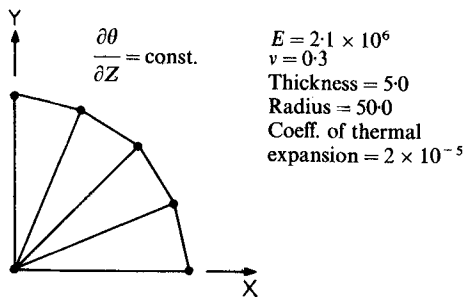


Figure 4. Simply-supported circular plate subjected to constant temperature gradient through the thickness. Four degenerated quadrilateral elements are used to model one-quarter of the plate. The finite element solution provides: (a) zero percent error in centre displacement; (b) zero stresses, coincident with the analytical solution

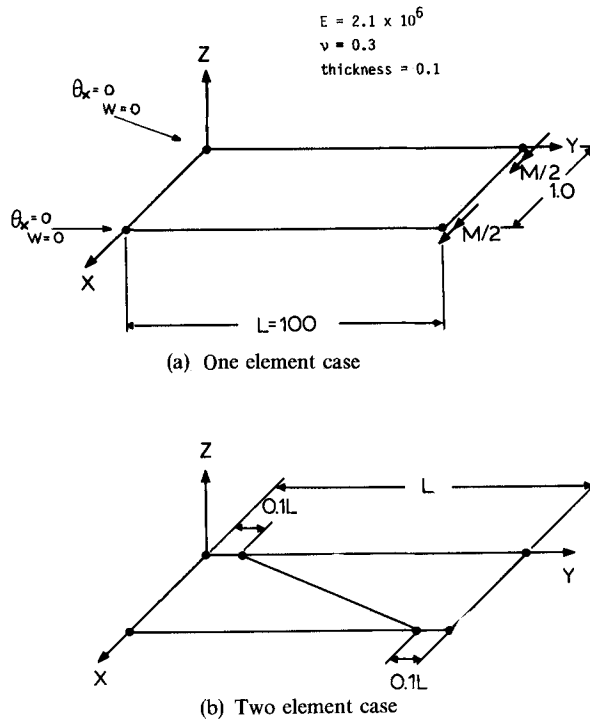
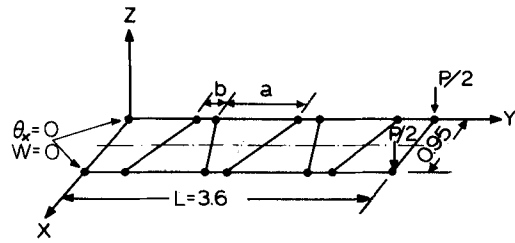


Figure 5. Cantilever subjected to tip bending moment. In both cases, the finite element solution for the displacements and rotations at the cantilever tip and for the stresses is coincident with the Bernoulli beam theory solution

modes because zero strains are calculated when the element nodal point displacements and rotations correspond to an element rigid body displacement, see equations (2)–(8).

2. *The element contains no spurious zero energy modes.* If the element were to contain a spurious zero energy mode, the strains along every side should vanish for a displacement pattern (to be identified) other than those corresponding to a true rigid body mode. However, such displacement pattern was not identified.

3. *The element passes the patch test and is applicable to the analysis of very thin plates (it does not 'lock').* See numerical solutions in Figures 3–11.



Error in displacements			$E = 2.0 \times 10^6$
a/b	$h/L = 1/10$	$h/L = 1/100$	
1.0	0.69%	0.69%	$\nu = 0.0$
5.0	1.58%	1.75%	Thickness = 0.36 and 0.036
58.0	2.57%	2.96%	$P = 100$
			Analyt. displ. = $\frac{PL^3}{3EI} + \frac{PL}{AG}$

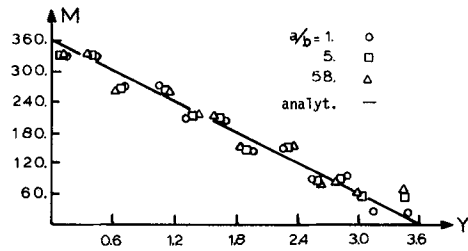
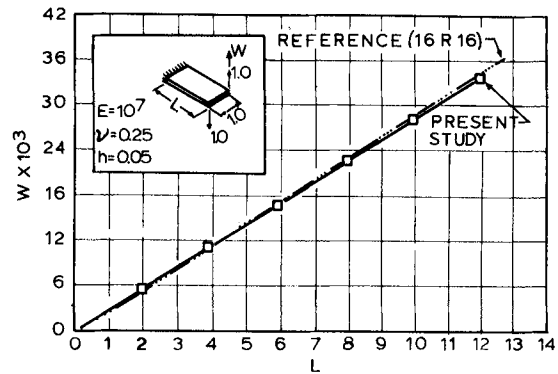
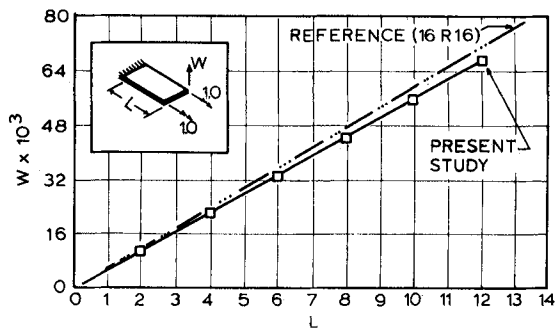


Figure 6. Cantilever under tip load. This problem was also analysed in Reference 5. The elements are distorted so as to keep their widths on the centreline constant. The moments are practically the same for both h/L ratios



(a) Twist case using differential loads



(b) Twist case using twisting moments

Figure 7. Single element results for twisting cases. The reference solution is given in Reference 10

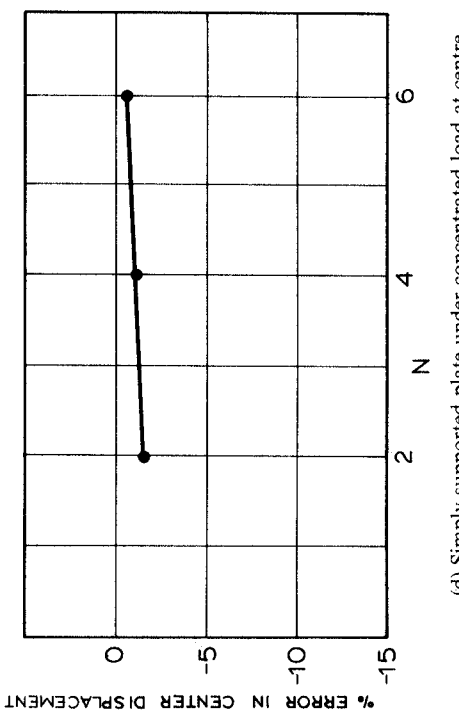
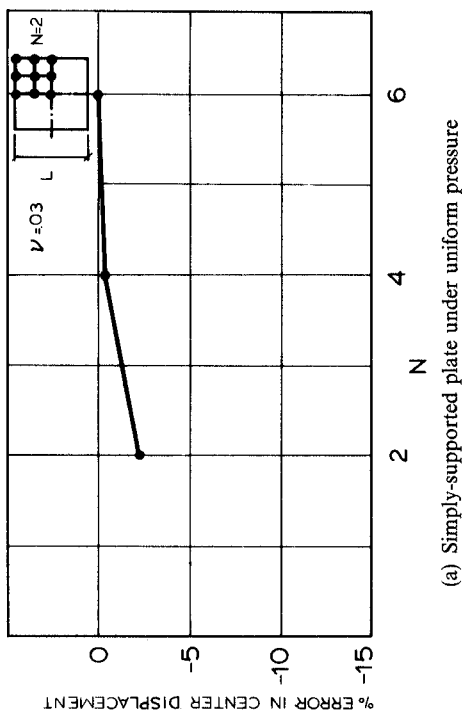
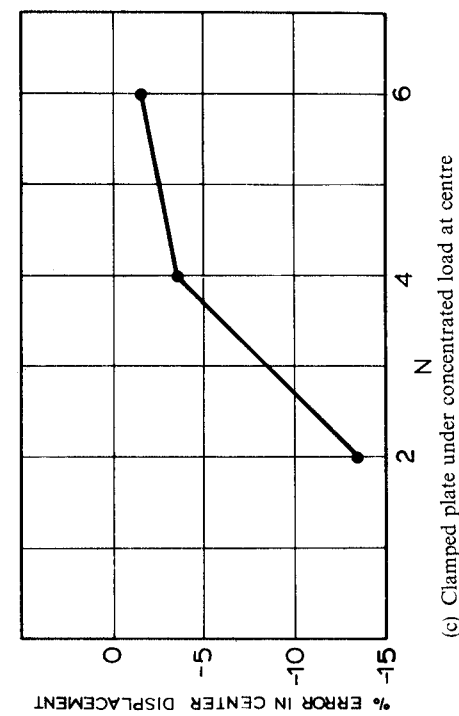
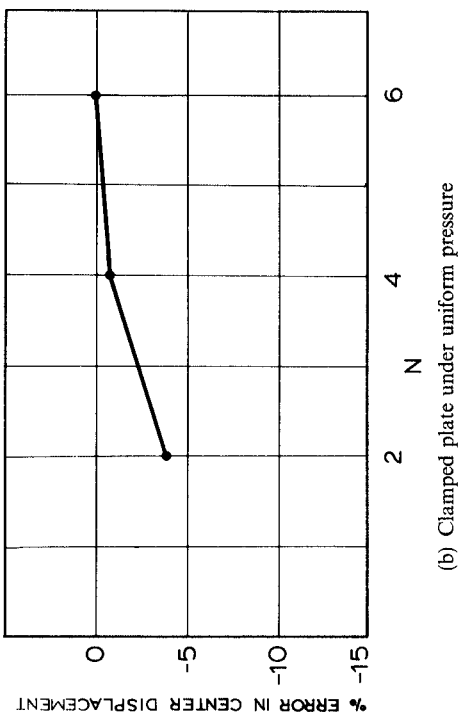


Figure 8. Predicted displacements in the analysis of a thin square plate ($L/h = 1000$). The finite element solution is compared with the Kirchhoff plate solution

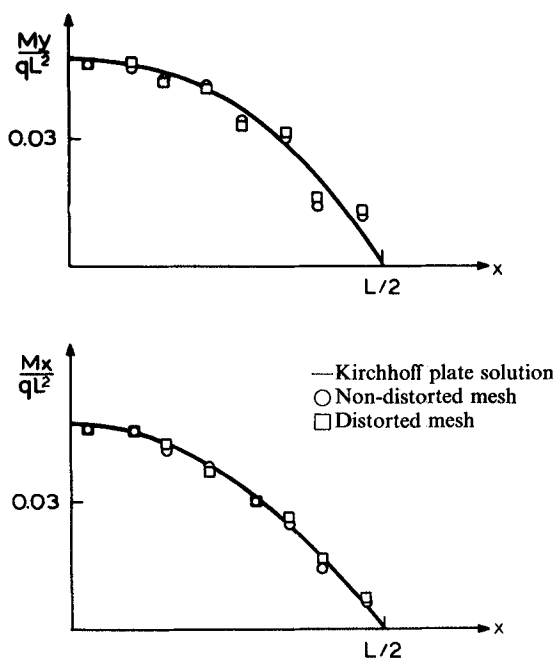
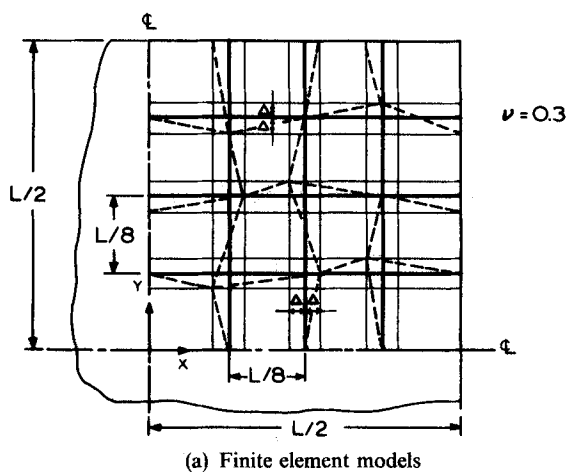
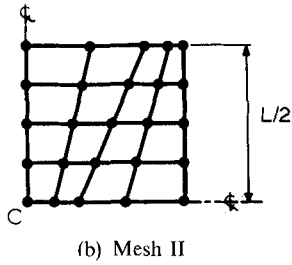
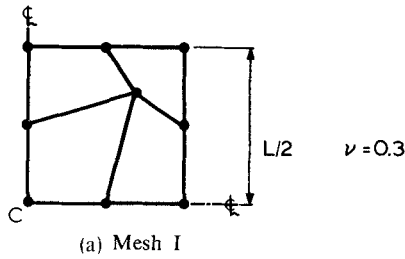


Figure 9. Bending moment distributions for thin simply-supported plate ($L/h = 1000$) under uniform pressure. The parameter of distortion, Δ , is equal to $L/40$

As regards the numerical integration we find that, even when the element is highly distorted, 2×2 standard Gauss integration is adequate.

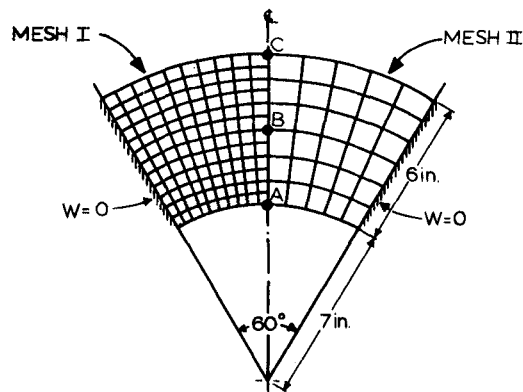
We have implemented the above element formulation by simply expanding the computer program QUADS given for plane stress analysis in Reference 2, p. 295. The complete program for the stiffness matrix calculations consists of about 150 lines.

Figures 3–11 show some analysis results obtained with our element. In these studies we consider



w^{FEM}	Mesh I	0.93
$w^{KIRCHHOFF}$	Mesh II	1.01
M^{FEM}	Mesh I	0.85
$M^{KIRCHHOFF}$	Mesh II	1.02

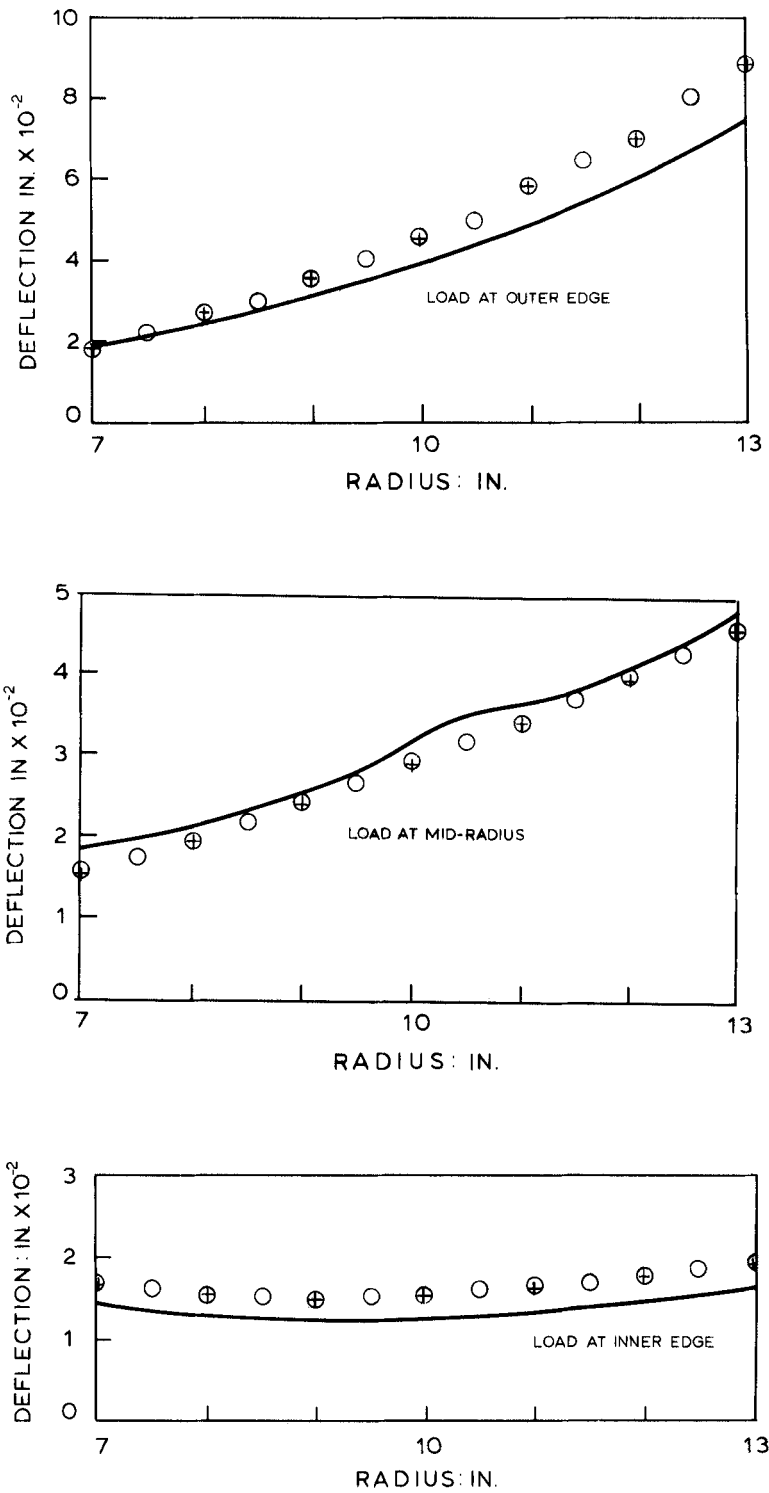
Figure 10. Effect of mesh distortion on results in analysis of a thin simply-supported plate under uniform pressure ($L/h = 1000$)



$E = 4.6 \times 10^5 \text{ lb/in}^2$; $\nu = 0.35$
 Thickness = 0.168 in

(a) Finite element mesh and data (ref. 3)

Figure 11. Analysis of a curved plate when subjected to a unit load at A (first load case), a unit load at B (second load case) and a unit load at C (third load case). The finite element results are compared with the analytical results obtained in Reference 11. The symbol \circ represents the results of mesh I, and the symbol $+$ represents the results of mesh II



(b) Solution results
Figure 11. (Continued)

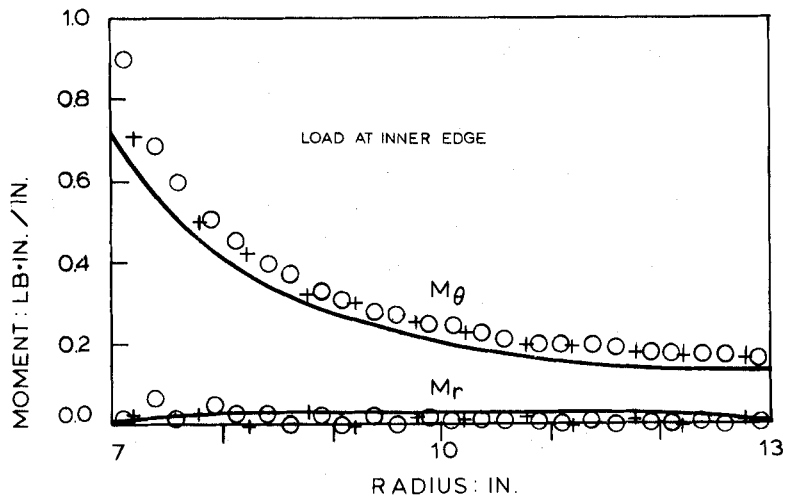
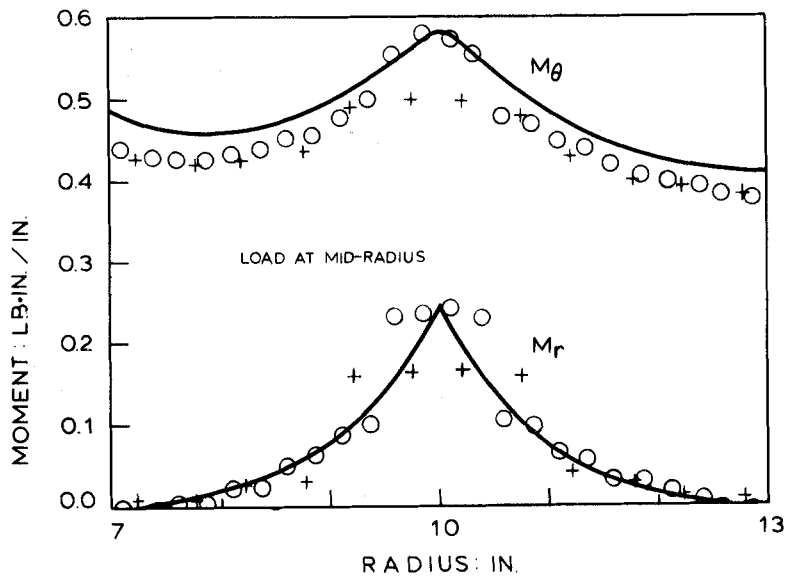
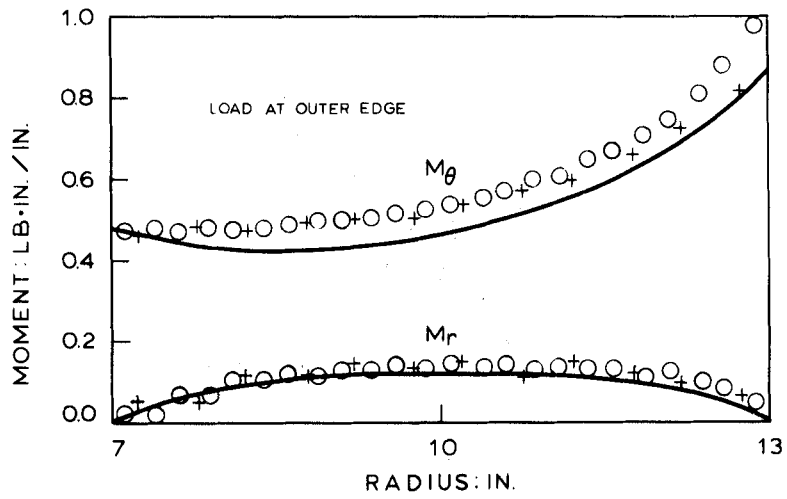


Figure 11(b). (Continued)

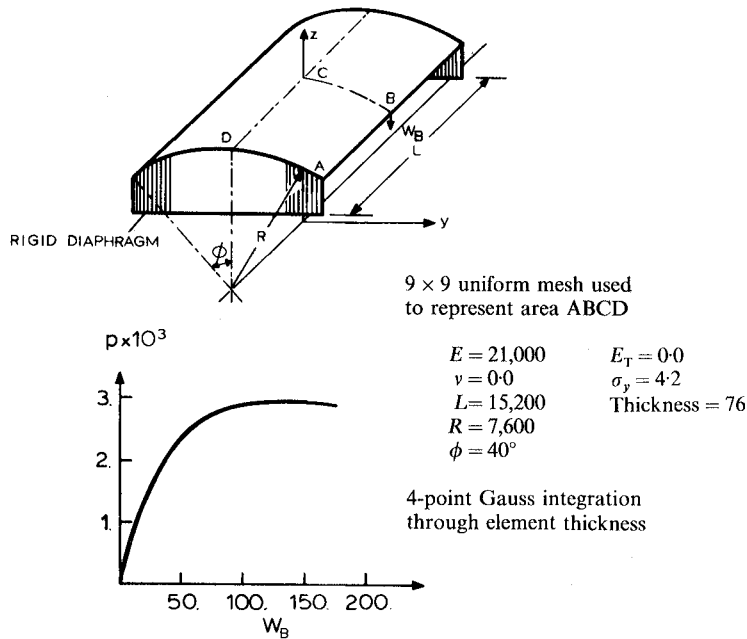


Figure 12. Large deflection elastic-plastic analysis of a cylindrical shell under constant vertical pressure loading per unit of projected area on the horizontal plane. In Reference 12 the solution (coincident with the present solution) is reported up to $w_B = 125$

only thin (and very thin) plate situations, in order to demonstrate the applicability of the element to such analyses, but the element can also be used for the analysis of moderately thick plates.⁴ The results show the convergence behaviour of the element in some problems and the effect of element distortions.

An important characteristic of the element is that it can only represent a constant bending moment exactly—but does so even when the element is highly distorted (see Figure 5). Therefore, to predict stress resultants accurately, a relatively fine mesh is needed in areas with large stress gradients (see Figure 11 for the load at point B).

Finally, to emphasize that this research was actually conducted to obtain a general nonlinear shell element, we present in Figure 12 the results of a geometric and material nonlinear shell solution obtained using the non-flat shell element of Reference 4.

CONCLUDING REMARKS

Our objective in this communication was to present in a compact manner a 4-node plate bending element that is obtained, as a special case, from a general 4-node shell element, and give further insight into the formulation of Reference 4. The continuum mechanics based approach used in the formulation has also much potential for the development of curved higher-order shell elements for general nonlinear analysis. These elements should also reduce to what should be attractive higher-order linear plate bending elements.

ACKNOWLEDGEMENTS

We are grateful for the financial support of the ADINA users' group for this work, and thank J. Dong of ADINA Engineering, Inc. for his help in some of the example analyses.

APPENDIX I: DERIVATION OF TRANSVERSE SHEAR INTERPOLATIONS

In the natural co-ordinate system of the plate bending element, the covariant base vectors are defined as¹³

$$\mathbf{g}_r = \frac{\partial \mathbf{x}}{\partial r}; \quad \mathbf{g}_s = \frac{\partial \mathbf{x}}{\partial s} \quad (11a)$$

$$\mathbf{g}_z = \frac{h}{2} \mathbf{e}_3 \quad (11b)$$

where \mathbf{x} is the vector of co-ordinates, $\mathbf{x} = x\mathbf{e}_1 + y\mathbf{e}_2$, and the \mathbf{e}_i are the base vectors of the Cartesian system.

The contravariant base vectors \mathbf{g}^i are defined by the following expression:

$$\mathbf{g}^i \cdot \mathbf{g}_j = \delta_j^i \quad (12)$$

where the δ_j^i are the mixed components of the Kronecker delta, and the i, j vary over r, s, z .

The following relations also hold:

$$g_{ij} = \mathbf{g}_i \cdot \mathbf{g}_j \quad (13a)$$

$$\mathbf{g}^i = g^{ij} \mathbf{g}_j \quad (13b)$$

$$g^{ij} = \frac{4D_{ij}}{h^2(\det \mathbf{J})^2} \quad (13c)$$

where D^{ij} is the cofactor of the term g_{ij} in the 3×3 matrix of the metric tensor.

In the natural co-ordinate system, the strain tensor can be expressed using covariant tensor components and contravariant base vectors,

$$\boldsymbol{\varepsilon} = \tilde{\varepsilon}_{ij} \mathbf{g}^i \mathbf{g}^j \quad (14)$$

where the tilde (\sim) indicates that the tensor components are measured in the natural co-ordinate system.

To obtain the shear tensor components we now use the equivalent of equation (6),

$$\tilde{\varepsilon}_{rz} = \frac{1}{2}(1+s)\tilde{\varepsilon}_{rz}^A + \frac{1}{2}(1-s)\tilde{\varepsilon}_{rz}^C \quad (15a)$$

$$\tilde{\varepsilon}_{sz} = \frac{1}{2}(1+r)\tilde{\varepsilon}_{sz}^D + \frac{1}{2}(1-r)\tilde{\varepsilon}_{sz}^B \quad (15b)$$

where $\tilde{\varepsilon}_{rz}^A$, $\tilde{\varepsilon}_{rz}^C$, $\tilde{\varepsilon}_{sz}^D$ and $\tilde{\varepsilon}_{sz}^B$ are the shear tensor components at points A, B, C and D . These quantities are evaluated using the linear terms of the relation¹³

$$\tilde{\varepsilon}_{ij} = \frac{1}{2} [{}^1\mathbf{g}_i \cdot {}^1\mathbf{g}_j - {}^0\mathbf{g}_i \cdot {}^0\mathbf{g}_j] \quad (16)$$

where the left superscript of the base vectors is equal to '1' for the deformed configuration and equal to '0' for the initial configuration. Substituting from equations (11) and equation (5) we obtain

$$\tilde{\varepsilon}_{rz}^A = \frac{1}{4} \left[\frac{h}{2}(w_1 - w_2) + \frac{h}{4}(x_1 - x_2)(\theta_y^1 + \theta_y^2) - \frac{h}{4}(y_1 - y_2)(\theta_x^1 + \theta_x^2) \right] \quad (17a)$$

and

$$\tilde{\varepsilon}_{rz}^C = \frac{1}{4} \left[\frac{h}{2}(w_4 - w_3) + \frac{h}{4}(x_4 - x_3)(\theta_y^4 + \theta_y^3) - \frac{h}{4}(y_4 - y_3)(\theta_x^4 + \theta_x^3) \right] \quad (17b)$$

Therefore, using equation (15a) we obtain

$$\begin{aligned} \tilde{\varepsilon}_{rz} = & \frac{1}{8}(1+s) \left[\frac{h}{2}(w_1 - w_2) + \frac{h}{4}(x_1 - x_2)(\theta_y^1 + \theta_y^2) - \frac{h}{4}(y_1 - y_2)(\theta_x^1 + \theta_x^2) \right] \\ & + \frac{1}{8}(1-s) \left[\frac{h}{2}(w_4 - w_3) + \frac{h}{4}(x_4 - x_3)(\theta_y^4 + \theta_y^3) - \frac{h}{4}(y_4 - y_3)(\theta_x^4 + \theta_x^3) \right] \end{aligned} \quad (18a)$$

and in the same way

$$\begin{aligned} \tilde{\varepsilon}_{sz} = & \frac{1}{8}(1+r) \left[\frac{h}{2}(w_1 - w_4) + \frac{h}{4}(x_1 - x_4)(\theta_y^1 + \theta_y^4) - \frac{h}{4}(y_1 - y_4)(\theta_x^1 + \theta_x^4) \right] \\ & + \frac{1}{8}(1-r) \left[\frac{h}{2}(w_2 - w_3) + \frac{h}{4}(x_2 - x_3)(\theta_y^2 + \theta_y^3) - \frac{h}{4}(y_2 - y_3)(\theta_x^2 + \theta_x^3) \right] \end{aligned} \quad (18b)$$

Next we use that

$$\tilde{\varepsilon}_{ij} \mathbf{g}^i \mathbf{g}^j = \varepsilon_{kl} \mathbf{e}_k \mathbf{e}_l \quad (19)$$

where the ε_{kl} are the components of the strain tensor measured in the Cartesian co-ordinate system.

From equation (19) we obtain

$$\gamma_{xz} = 2\tilde{\varepsilon}_{rz}(\mathbf{g}^r \cdot \mathbf{e}_x)(\mathbf{g}^z \cdot \mathbf{e}_z) + 2\tilde{\varepsilon}_{sz}(\mathbf{g}^s \cdot \mathbf{e}_x)(\mathbf{g}^z \cdot \mathbf{e}_z) \quad (20a)$$

$$\gamma_{yz} = 2\tilde{\varepsilon}_{rz}(\mathbf{g}^r \cdot \mathbf{e}_y)(\mathbf{g}^z \cdot \mathbf{e}_z) + 2\tilde{\varepsilon}_{sz}(\mathbf{g}^s \cdot \mathbf{e}_y)(\mathbf{g}^z \cdot \mathbf{e}_z) \quad (20b)$$

But

$$\mathbf{g}^r = \sqrt{g^{rr}}(\sin \beta \mathbf{e}_x - \cos \beta \mathbf{e}_y) \quad (21a)$$

$$\mathbf{g}^s = \sqrt{g^{ss}}(-\sin \alpha \mathbf{e}_x + \cos \alpha \mathbf{e}_y) \quad (21b)$$

$$\mathbf{g}^z = \sqrt{g^{zz}} \mathbf{e}_z \quad (21c)$$

where α and β are the angles between the x - and r -axis and x - and s -axis, respectively.

Also, using equations (13)

$$g^{rr} = \frac{(C_x + rB_x)^2 + (C_y + rB_y)^2}{16(\det \mathbf{J})^2} \quad (22a)$$

$$g^{ss} = \frac{(A_x + sB_x)^2 + (A_y + sB_y)^2}{16(\det \mathbf{J})^2} \quad (22b)$$

where the A_x , B_x , C_x , A_y , B_y and C_y are defined in equations (10), and

$$g^{zz} = \frac{4}{h^2} \quad (22c)$$

Substituting from equations (18), (21) and (22) into equations (20), the relations in equations (8) are obtained.

REFERENCES

1. O. C. Zienkiewicz, *The Finite Element Method*, McGraw-Hill, 1977.
2. K. J. Bathe, *Finite Element Procedures in Engineering Analysis*, Prentice-Hall, 1982.
3. J.-L. Batoz and M. Ben Tahar, 'Evaluation of a new quadrilateral thin plate bending element', *Int. j. numer. methods eng.*, **18**, 1655-1677 (1982).
4. E. N. Dvorkin and K. J. Bathe, 'A continuum mechanics based four-node shell element for general nonlinear analysis', *Eng. Comput.*, **1**, 77-88 (1984).

5. R. H. MacNeal, 'Derivation of element stiffness matrices by assumed strain distributions', *Nucl. Eng. Design*, **70**, 3–12 (1982).
6. T. J. R. Hughes and T. E. Tezduyar, 'Finite elements based upon Mindlin plate theory with particular reference to the four-node bilinear isoparametric element', *ASME, J. Appl. Mech.*, **46**, 587–596 (1981).
7. J.-L. Batoz, K. J. Bathe and L. W. Ho, 'A study of three-node triangular plate bending elements', *Int. j. numer. methods eng.*, **15**, 1771–1812 (1982).
8. K. J. Bathe, E. N. Dvorkin and L. W. Ho, 'Our discrete—Kirchhoff and isoparametric shell elements for nonlinear analysis—an assessment', *J. Computers Struct.*, **16**(1–4), 89–98 (1983).
9. M. Bercovier, Y. Hasbani, Y. Gilon and K. J. Bathe, 'On a finite element procedure for nonlinear incompressible elasticity', in *Hybrid and Mixed Finite Element Methods* (Eds. S. N. Atluri *et al.*), Wiley, 1983.
10. J. Robinson and G. W. Haggemacher, 'LORA—an accurate four node stress plate bending element', *Int. j. numer. methods eng.*, **14**, 296–306 (1979).
11. A. Coull and P. C. Das, 'Analysis of curved bridge decks', *Proc. Inst. Civ. Eng., Lond.*, **37**, 75–85 (1967).
12. B. Kråkeland, 'Nonlinear analysis of shells using degenerate isoparametric elements', in *Finite Elements in Nonlinear Mechanics*, vol. 1 (Eds. P. G. Bergan *et al.*), Tapir Publishers, Norwegian Institute of Technology, Trondheim, Norway, 1978.
13. A. E. Green and W. Zerna, *Theoretical Elasticity*, 2nd edn, Oxford University Press, 1968.